Depolarizing GABA Transmission Restrains Activity-Dependent Glutamatergic Synapse Formation in the Developing Hippocampal Circuit

Short Title: GABA Restrains Excitatory Synapse Formation

Christopher K. Salmon[1], Horia Pribiag[1], W. Todd Farmer[1], Scott Cameron[1], Emma V. Jones[1], Vivek Mahadevan[2], David Stellwagen[1], Melanie A. Woodin[2], and Keith K. Murai[1*]

[1]Centre for Research in Neuroscience, Department of Neurology and Neurosurgery, The Research Institute of the McGill University Health Centre, Montreal General Hospital, Montreal, Quebec, H3G 1A4, Canada.

[2]Department of Cell & Systems Biology, University of Toronto, Toronto, Ontario, M5S 3G5, Canada.

[*]Correspondence should be addressed to:
Dr. Keith K. Murai
Centre for Research in Neuroscience
Montreal General Hospital
1650 Cedar Avenue L7-212
Montreal, QC, H3G 1A4 Canada
Telephone: (514) 934-1934 x43477
Fax: (514) 934-8216
keith.murai@mcgill.ca

Number of figures: 4
Supplementary figures: 5
Number of words: 8631 (Abstract 285; Intro 641; Discussion 1563)

Key Words: Synapse formation, hippocampus, GABA transmission, dendritic spines, chloride homeostasis, KCC2, circuit development, autism

Acknowledgements: The authors would like to thank Dr. Andrew Greenhalgh and Andy YL Gao for critical review of the manuscript. This work was supported by the Canadian Institutes of Health Research (M.A.W and K.K.M) and Natural Sciences and Engineering Research Council of Canada (K.K.M). C.K.S. was supported through a CGS-M from the CIHR and a Doctoral Award from the FRQS. The authors declare no competing financial interests.

ABSTRACT

GABA is the main inhibitory neurotransmitter in the mature brain but has the paradoxical property of depolarizing neurons during early development. Depolarization provided by $GABA_A$ transmission during this early phase regulates neural stem cell proliferation, neural migration, neurite outgrowth, synapse formation, and circuit refinement, making GABA a key factor in neural circuit development. Importantly, depending on the context, depolarizing $GABA_A$ transmission can either drive neural activity, or inhibit it through shunting inhibition. The varying roles of depolarizing $GABA_A$ transmission during development, and its ability to both drive and inhibit neural activity, makes it a difficult developmental cue to study. This is particularly true in the later stages of development, when the majority of synapses form and $GABA_A$ transmission switches from depolarizing to hyperpolarizing. Here we addressed the importance of depolarizing but inhibitory (or shunting) $GABA_A$ transmission in glutamatergic synapse formation in hippocampal CA1 pyramidal neurons. We first showed that the developmental depolarizing-to-hyperpolarizing switch in $GABA_A$ transmission is recapitulated in organotypic hippocampal slice cultures. Based on the expression profile of K^+-Cl^- co-transporter 2 (KCC2) and changes in the GABA reversal potential, we pinpointed the timing of the switch from depolarizing to hyperpolarizing $GABA_A$ transmission in CA1 neurons. We found that blocking depolarizing but shunting $GABA_A$ transmission increased excitatory synapse number and strength, indicating that depolarizing $GABA_A$ transmission can restrain glutamatergic synapse formation. The increase in glutamatergic synapses was activity-dependent, but independent of BDNF signalling. Importantly, the elevated number of synapses was stable for more than a week after $GABA_A$ inhibitors were washed out. Together these findings point to the ability of immature GABAergic transmission to restrain glutamatergic synapse formation and suggest an unexpected role for depolarizing $GABA_A$ transmission in shaping excitatory connectivity during neural circuit development.

INTRODUCTION

γ-Aminobutyric acid (GABA) is the main inhibitory neurotransmitter in the mature brain. However, GABA is paradoxically depolarizing during nervous system development. Many *in vitro* studies in rodents have shown that depolarizing $GABA_A$ transmission

provides excitatory drive during gestation and early postnatal CNS development, driving early network oscillations (ENOs) thought to promote activity-dependent maturation of neural circuits (Ben-Ari et al., 2012). However, recent work suggests that despite providing local depolarization, immature $GABA_A$ transmission has inhibitory effects *in vivo* (Kirmse et al., 2015; Oh et al., 2016; Valeeva et al., 2016). This ability of GABA to be simultaneously depolarizing and inhibitory relies on shunting inhibition, which results from a decrease in input resistance and membrane time constant when $GABA_A$ receptors open, regardless of the direction of Cl^- flux (Staley and Mody, 1992). Importantly, shunting inhibition can occur in conjunction with both hyperpolarizing and depolarizing $GABA_A$ transmission, and we therefore refer to the latter case as depolarizing/inhibitory.

Depolarizing $GABA_A$ transmission is implicated in numerous neurodevelopmental processes in vertebrates, including neural stem cell proliferation (Liu et al., 2005), cell migration (Behar et al., 2000), neurite outgrowth (Cancedda et al., 2007), synapse formation, and circuit refinement (Akerman and Cline, 2006; Cancedda et al., 2007; Wang and Kriegstein, 2008). Critically, circuit activity supported by depolarizing $GABA_A$ transmission *in vitro* drives calcium influx thought to be important for glutamatergic synapse development (Leinekugel et al., 1995; Ben-ari et al., 1997; Griguoli and Cherubini, 2017). Indeed, disrupting the depolarizing nature of $GABA_A$ transmission by interfering with chloride homeostasis alters glutamatergic synapse formation and maturation (Akerman and Cline, 2006; Wang and Kriegstein, 2008). However, the effects of $GABA_A$ transmission itself on glutamatergic synapse development and the timing of these effects remain poorly defined. This is partly due to the difficulty in manipulating depolarizing $GABA_A$ transmission in defined cell types and circuits with sufficient temporal resolution to specifically target the period when glutamatergic synapses are forming, while sparing the preceding developmental roles of GABA. Several studies have prematurely hyperpolarized the reversal potential for chloride (E_{Cl}) by disrupting chloride homeostasis for more than a week during perinatal development, across a timespan in which the targeted neurons terminally divide, migrate, extend neurites and are incorporated into the surrounding circuitry (Ge et al., 2006; Cancedda et al., 2007; Wang and Kriegstein, 2008). This work suggests that disrupting E_{Cl} alters neurite and synapse maturation, however, it has been noted that additional studies with higher temporal resolution are needed

(Akerman and Cline, 2007; Kirmse et al., 2018). Closing this gap in our understanding of how $GABA_A$ transmission and its transition from a depolarizing to a hyperpolarizing state impacts glutamatergic synapse development will help solve a now classic problem in developmental neurobiology, and will likely be of clinical significance as disruptions of $GABA_A$ transmission during brain development are associated with neurodevelopmental disorders (El Marroun et al., 2014; He et al., 2014; Tyzio et al., 2014).

Here we investigated the role of depolarizing $GABA_A$ transmission in glutamatergic synapse formation on hippocampal CA1 pyramidal cells. To perform temporally precise pharmacological manipulations of $GABA_A$ transmission during neural circuit development, we took advantage of the properties of the organotypic hippocampal slice culture. This preparation preserves the anatomy and the developmental progression of the hippocampus, including the time course of excitatory synapse formation (Buchs et al., 1993; Muller et al., 1993; De Simoni et al., 2003). This system enabled us to define a narrow time window during the first week of slice development in which $GABA_A$ transmission shifts from immature, depolarizing transmission, to hyperpolarizing transmission in CA1 pyramidal cells. Previous work suggests that blocking depolarizing $GABA_A$ transmission during development will remove excitatory drive and decrease excitatory synapse formation and maturation (Ben-Ari et al., 2007; Wang and Kriegstein, 2008). Contrary to these predictions, we found that transient blockade of immature, depolarizing $GABA_A$ transmission increased glutamatergic synapse number and function on CA1 pyramidal cells. This unexpected effect was explained by the finding that, at this stage of development, depolarizing $GABA_A$ transmission provides shunting inhibition, which when blocked alleviated a restraint on activity-dependent synapse formation. Interestingly, the activity-dependent increase in glutamatergic synapses was stable for at least a week. Furthermore, the effect could not be reproduced by prematurely hyperpolarizing E_{GABA}, and was independent of BDNF signalling. Our results therefore point to an important time window during hippocampal development when immature $GABA_A$ transmission can restrain excitatory synapse development, and that interfering with $GABA_A$ transmission at this stage can have lasting effects on neural circuitry.

RESULTS

$GABA_A$ transmission switches from depolarizing to hyperpolarizing in CA1 cells during the first week in hippocampal slice culture.

Depolarizing $GABA_A$ transmission relies on relatively high intracellular chloride ($[Cl^-]_i$). As neurons mature during the first weeks of postnatal CNS development, Na^+-K^+-Cl^- cotransporter (NKCC1) expression is downregulated and K^+-Cl^- cotransporter 2 (KCC2) is upregulated, lowering $[Cl^-]_i$ (Rivera et al., 1999; Yamada et al., 2004). $GABA_A$ receptors are largely permeable to Cl^-, and to a lesser extent bicarbonate (HCO_3^-) (Kaila, 1994; Staley and Proctor, 1999). When $[Cl^-]_i$ lowers to the point at which the reversal potential for GABA (E_{GABA}) hyperpolarizes below the resting membrane potential, $GABA_A$ transmission switches from depolarizing to hyperpolarizing. To pinpoint when this switch from depolarization to hyperpolarization occurs in CA1 pyramidal cells in hippocampal organotypic slices, we first assessed the timing of KCC2 upregulation across the first two weeks *in vitro* and found expression of both KCC2 monomers (KCC2-M) and oligomers (KCC2-O) underwent a large and graded increase between 3 and 7DIV (Fig 1A,B), reaching near-maximal levels by 7 days *in vitro* (DIV) (Fig 1B). Using this timeframe as a guide, we performed gramicidin perforated patch recordings to determine the $GABA_A$ reversal potential (E_{GABA}) in CA1 pyramidal cells (exemplary traces and IV curves shown in Figures 1C and D). At 3-4 DIV, E_{GABA} was depolarized with respect to resting membrane potential (RMP) (Fig 1E-G). However, by 6-7 DIV E_{GABA} was hyperpolarized with respect to RMP, indicating a switch to hyperpolarizing $GABA_A$ transmission by 6-7 DIV (Fig 1C-G), a timeframe similar to that reported previously for CA1 pyramidal cells (Swann et al., 1989). E_{GABA} was more negative than action potential threshold at 3-4 DIV (Fig 1E,G), suggesting GABA is depolarizing but not capable of directly depolarizing neurons past action potential (AP) threshold from rest at this stage.

Blocking depolarizing $GABA_A$ transmission increases CA1 spine density.

Overexciting mature neurons by blocking hyperpolarizing $GABA_A$ transmission is known to cause a collapse of dendritic spines both *in vivo* (Zeng et al., 2007) and *in vitro* (Muller et al., 1993; Drakew et al., 1996; Jourdain et al., 2002; Zha et al., 2005). In particular, applying $GABA_A$ antagonists to organotypic hippocampal cultures at 5 or 23 DIV over a period of 2 to 3 days was shown to cause a robust loss of spines (Drakew et

al., 1996; Zha et al., 2005). Consistent with this, when we blocked $GABA_A$ transmission with the $GABA_AR$ antagonist, bicuculline (BIC) from 5-7 DIV (when $GABA_A$ transmission is hyperpolarizing (Fig 1C-H)), spine density decreased by 34% (Fig 2A-C). This suggests that by this stage, excitatory transmission causes overexcitation and spine loss in the absence of hyperpolarizing $GABA_A$ transmission.

To assess the role of immature, depolarizing $GABA_A$ transmission on dendritic spine development, we inhibited $GABA_A$ transmission earlier, from 3-5 DIV (Fig 2D). Previous work suggests that inhibiting depolarizing $GABA_A$ transmission during development would decrease glutamatergic synapse formation and maturation (Ben-ari et al., 1997; Hanse et al., 1997; Cancedda et al., 2007; Wang and Kriegstein, 2008). However, in contrast to these findings, BIC applied for 48 hours from 3 to 5 DIV significantly increased dendritic spine density (25% increase)(Fig 2E-F). This effect was fully reproducible with the $GABA_AR$ antagonist gabazine (GBZ)(31% increase)(Fig 2E,G), which is a more specific antagonist of $GABA_ARs$ (Heaulme et al., 1986) and blocks inhibition more consistently in hippocampal neurons (Sokal et al., 2000). We also verified that the presence of penicillin-streptomycin in the culture medium was not associated with this effect by blocking GABA transmission in the absence antibiotics, and found the same increase in dendritic spines (S1A-C Fig).

To assess whether the supernumerary spines induced by blocking depolarizing $GABA_A$ transmission showed structural differences, we analyzed spine morphology. GBZ treatment did not affect the proportions of mushroom, thin, and stubby spines (Fig 2H), 2-dimensional head area (Control: 0.32±0.02 μm^2; GBZ: 0.37±0.04 μm^2, $p>0.10$), head diameter (Control: 0.58±0.02 μm^2; GBZ: 0.62±0.03 μm^2, $p>0.1$), spine length (Control 1.66±0.09 μm^2; GBZ: 1.83±0.08 μm^2, $p>0.1$) or dendrite diameter (Fig 2I).

We next asked whether the increased number of spines constituted an increase in *bona fide* glutamatergic synapses on CA1 cells by recording miniature EPSCs (mEPSC). Consistent with the increase in dendritic spine density, mEPSC analysis showed that GBZ treatment (3-5 DIV) increased mESPC frequency 3-fold (Fig 2J,K). Miniature EPSC amplitude also increased, indicating enhanced synaptic strength (Fig 2L-M). Together, these results suggest that immature $GABA_A$ transmission restrains glutamatergic synapse formation and maturation.

The narrow time window we examined raised the possibility that the spine-enhancing effect of $GABA_A$ blockade is limited to a short period directly prior to the depolarizing to hyperpolarizing shift in $GABA_A$ transmission. This would suggest that $GABA_A$ transmission restrains glutamatergic synapse formation only during a very short transition state. To test whether this was the case, we prepared slices 3 days earlier (P2) and applied GBZ at 3DIV for 48h (S1D Fig). We found that $GABA_AR$ blockade in these younger slices also caused a significant increase in spines (S1E,F Fig), suggesting that depolarizing $GABA_A$ transmission is capable of restraining synapse formation for an appreciable period during postnatal development.

Bumetanide treatment has no effect on spine numbers.

Previous work suggests that abrogating GABAergic depolarization by prematurely rendering GABA hyperpolarizing decreases glutamatergic synapse formation (Ge et al., 2006; Wang and Kriegstein, 2008). However, our data show that a complete loss of depolarizing $GABA_A$ transmission increases glutamatergic synapse formation. These contrasting results raise the question of whether the depolarizing nature of $GABA_A$ transmission is important for the normal development of glutamatergic synapse number in our period of interest (3-5 DIV). To address this, we asked whether prematurely hyperpolarizing E_{GABA} could mimic the effect of $GABA_A$ blockade by treating slices with the NKCC1 blocker bumetanide (BUME) from 3 to 5DIV (S2 Fig). BUME is well established to lower E_{GABA} in immature neurons (Dzhala et al., 2005) and prematurely render GABA hyperpolarizing (Wang and Kriegstein, 2011). Treating slice cultures at 3DIV with BUME did not alter spine density on its own (S2A,B Fig), indicating that the depolarizing nature of GABA is not important for regulating spine numbers at this stage of development. Furthermore, BUME did not alter the effect of GBZ on spine density, indicating that the extent to which E_{GABA} is depolarized is not important for limiting spine density to normal levels at this stage.

Since KCC2 overexpression can cause an increase in spines through its non-transport, scaffolding function (Li et al., 2007; Fiumelli et al., 2012), we also assessed KCC2 expression following GBZ treatment. GBZ did not significantly elevate expression of KCC2 oligomers or monomers (S2C-E Fig).

Driving depolarizing $GABA_A$ transmission does not alter glutamatergic synapse number.

Next, we investigated if increasing $GABA_A$ transmission over the 3-5 DIV period would have the opposite effect to GABA-blockade and reduce excitatory synapses. Previous work has demonstrated that propofol, a positive allosteric modulator of $GABA_A$Rs, decreases spine density in developing layer 2/3 principal cells of the somatosensory cortex when administered to rat pups over a 6h period at postnatal day 10, when $GABA_A$ transmission is still depolarizing (Puskarjov et al., 2017). To test this in CA1 pyramidal cells, we increased depolarizing $GABA_A$ transmission by administering muscimol (MUS) or diazepam (DZP) from 3 to 5DIV. MUS treatment did not significantly decrease spine density (S3A-C Fig). Furthermore, mEPSC frequency was unchanged, confirming MUS did not alter synapse numbers (S3D,E Fig). MUS has varying effects on different GABA receptors and can cause $GABA_A$ receptor desensitization, making its effects difficult to interpret (Heck et al., 2007; Mortensen et al., 2010; Johnston, 2014). We therefore also tested whether enhancing $GABA_A$ transmission with DZP could decrease glutamatergic synapses, but this also had no effect on spine density or mEPSCs (S3A-F Fig). Based on these results, increasing $GABA_A$ transmission was not sufficient to decrease glutamatergic synapse number or function, suggesting depolarizing $GABA_A$ transmission can only limit synapse formation up to a certain point at this stage of development. However, our results do not rule out the possibility that enhancing immature $GABA_A$ transmission on different timescales or in other systems decreases glutamatergic synapse formation (Puskarjov et al., 2017).

Increased glutamatergic synapses following blockade of depolarizing $GABA_A$ transmission is activity-dependent.

Based on our recordings showing that at 3-4DIV E_{GABA} is depolarized relative to RMP, but lower than action potential threshold (Fig 1E-G), GABA is likely to mediate shunting inhibition (ie depolarizing/inhibitory transmission), at this stage (see S4A Fig for schematic). To test this possibility, we puffed GABA locally while recording spontaneous or electrically evoked firing. GABA inhibited both spontaneous (Fig 3A,B) and evoked spiking (S1B,C Fig), suggesting that although E_{GABA} is depolarizing relative to RMP,

$GABA_A$ transmission is inhibitory during the 3-5 DIV timeframe. Blocking this depolarizing/inhibitory $GABA_A$ transmission likely increased activity in our preparation, suggesting that the increase in glutamatergic synapses following GABA-blockade at 3DIV may be driven by activity-dependent mechanisms (Balkowiec and Katz, 2002; Pérez-Gómez and Tasker, 2013). To address this hypothesis, we measured levels of *Bdnf* and *Fos* mRNA, two activity regulated genes associated with glutamatergic synapse formation (Vicario-Abejón et al., 1998, 2002; Tyler and Pozzo-Miller, 2003; Chapleau et al., 2009). Both transcripts were significantly upregulated following 48-hour blockade of depolarizing/inhibitory $GABA_A$ transmission (*Bdnf*: 5-fold increase, *Fos*: 2.5-fold increase) (Fig 3C). $GABA_A$ blockade at 3DIV also increased Fos protein expression after 24 and 48 hours (Fig 3D-E). Together these data indicate that blocking immature depolarizing $GABA_A$ transmission at this point caused an increase in activity in CA1 pyramidal cells. To test whether the increased synapse formation we observed following GABA blockade at 3DIV was activity-dependent, we treated slice cultures with GBZ and/or TTX, and found that while TTX alone had no effect on spine density, TTX blocked the GBZ-induced increase in spines (Fig 3F). From this we conclude that depolarizing/inhibitory $GABA_A$ limits activity-dependent glutamatergic synapse formation at this point in the development of hippocampal circuitry in slice culture.

BDNF is known to regulate activity-dependent synapse formation and plasticity (Park and Poo, 2013), and we therefore asked whether BDNF signaling was responsible for the increase in spines following blockade of depolarizing/inhibitory $GABA_A$ transmission. We inhibited BDNF signalling during the 3 to 5DIV GBZ treatment using TrkB-Fc bodies or K252a (Ji et al., 2010; Puskarjov et al., 2014), however neither approach blocked the increase in spine density (Fig 3G,H), suggesting that BDNF signalling is not necessary for the observed increase in spines.

Blocking depolarizing $GABA_A$ transmission leads to a sustained increase in glutamatergic synapses.

The observed increase in spine density induced by blocking depolarizing/inhibitory $GABA_A$ transmission may only lead to a transient alteration without a longer lasting effect on glutamatergic synapses. To determine whether blockade of $GABA_A$ transmission caused a temporary or sustained increase in glutamatergic synapses, we treated slices

with GBZ from 3-5 DIV and allowed them to recover for an additional 5-9 days in the absence of GBZ (Fig 4A). This temporary $GABA_A$ blockade resulted in a 37% increase in spine density after a 5-day recovery period (Fig 4B,C). Furthermore, after this recovery period, CA1 cells had more thin spines than mushroom spines, a difference not present in the control condition (Fig 4D). No changes in dendrite diameter were observed (Fig 4E). To determine if transient GBZ treatment led to long-term functional changes in glutamatergic synapses, we recorded mEPSC frequency and amplitude after 8-9 days of recovery. We found that mEPSC frequency was enhanced by 79%, while mEPSC amplitude was unchanged at this stage (Fig 4F-I). Together these data suggest that inhibiting depolarizing $GABA_A$ transmission during a narrow time window can lead to persistent changes in glutamatergic synapse number in the hippocampus.

DISCUSSION

Immature, depolarizing $GABA_A$ transmission is believed to promote glutamatergic synapse formation and maturation (Ben-ari et al., 1997; Hanse et al., 1997; Wang and Kriegstein, 2009; Chancey et al., 2013). However, when and how GABA affects glutamatergic synapse formation remains to be fully understood. Indeed, several groups have noted that tools and approaches for manipulating depolarizing $GABA_A$ transmission with higher temporal and spatial precision are needed to resolve this (Akerman and Cline, 2007; Chancey et al., 2013; Kirmse et al., 2018). We therefore sought to address the role of $GABA_A$ transmission in glutamatergic synapse formation by performing precisely timed pharmacological manipulations in hippocampal slice cultures. We first mapped the depolarizing-to-hyperpolarizing shift of $GABA_A$ transmission in CA1 cells. This was followed by structural and electrophysiological analysis which showed that blocking immature, depolarizing/inhibitory $GABA_A$ transmission enhanced glutamatergic synapse function and number. Interestingly, the enhanced synapse number was stable following a recovery period. These results suggest that immature $GABA_A$ transmission restrains glutamatergic synapse formation during an early phase of hippocampal circuit development. Using slice cultures allowed for more temporally precise manipulations that revealed this effect, though limitations of this model system must be considered when interpreting our results. In particular, exuberant glutamatergic synapse formation has

been observed in slice cultures, and has been attributed to increases in distal dendritic branching (De Simoni et al., 2003). However, we minimized this confound by focusing on primary apical dendrites, which are fully formed by the time of pharmacological treatment. Thus, while further work will be required to extend our findings to other systems, the results of this study show that immature, depolarizing $GABA_A$ transmission is capable of restraining glutamatergic synapse formation in certain contexts, and that the removal of this restraint by interfering with $GABA_A$ transmission during development may cause a long-term increase in glutamatergic synapses.

An unpredicted role for immature $GABA_A$ transmission in restraining glutamatergic synapse formation

In the time window we examined, $GABA_A$ transmission provides subthreshold depolarization and shunting inhibition, which when blocked alleviates a brake on glutamatergic synapse development. Taken in the context of previous work, our results suggest a couple of models for how immature $GABA_A$ transmission affects hippocampal excitatory connectivity (S5 Fig). Firstly, the GABA-mediated restraint on glutamatergic synapse formation may be a short-lived feature of a depolarizing/inhibitory transition state that GABA passes through as E_{Cl} matures from depolarizing and excitatory to hyperpolarizing (Model 1, S5A-C Fig). However, recent work suggests GABA may be inhibitory throughout most or all of postnatal development. Therefore, in a second model, depolarizing but inhibitory $GABA_A$ transmission may inhibit circuit activity from birth onward (Model 2, S5B-C Fig), thus restraining glutamatergic synapse formation across development.

The first model is based on evidence from acute slices suggesting that immature $GABA_A$ transmission is capable of driving excitation (Gulledge and Stuart, 2003) and that depolarizing $GABA_A$ transmission drives ENOs, which in turn promote glutamatergic synapse formation and unsilencing, and circuit refinement (Hanse et al., 1997; Ben-Ari, 2002; Wang and Kriegstein, 2009; Griguoli and Cherubini, 2017). Disrupting E_{Cl} or $GABA_A$ transmission in this phase of development is hypothesized to interfere with synapse formation (S5A Fig), and this has been borne out by experimentally lowering E_{Cl} across the postmitotic period in immature neurons (Ge et al., 2006; Cancedda et al., 2007; Wang

and Kriegstein, 2008). Incorporating our results refines this model and accounts for the role of $GABA_A$ transmission in circuit development as it transitions from a depolarizing and excitatory to a hyperpolarizing state. Our work suggests that following an initial depolarizing phase in which GABA promotes excitation, as E_{Cl} progressively matures, $GABA_A$ transmission passes through a transient but developmentally relevant depolarizing/inhibitory phase (S5B Fig). Such a transition phase is hinted at in the literature, as certain studies have shown that blocking depolarizing $GABA_A$ transmission can silence ENOs, while others show $GABA_A$ blockade to increase circuit activity by eliciting interictal discharges or paroxysmal activity (Le Magueresse et al., 2006; Ben-Ari et al., 2007). Our results suggest that during this transition phase, depolarizing $GABA_A$ transmission is inhibitory and restrains glutamatergic synapse formation. Blocking $GABA_A$ transmission at this time alleviates the restraint, allowing for activity-dependent synapse formation (S5B Fig). Following this transition phase, $GABA_A$ transmission becomes fully hyperpolarizing as the glutamatergic system becomes capable of overexcitation. The result of $GABA_A$ blockade at this stage is loss of spines (Fig 2 and S5C Fig) (Swann et al., 1989; Drakew et al., 1996; Zeng et al., 2007). Interestingly, the absence of a similar spine loss following blockade of depolarizing/inhibitory $GABA_A$ transmission at 3DIV suggests that, while this still immature GABAergic inhibition is important for regulating activity levels, the glutamatergic system is not yet mature enough to cause a pathological collapse of synapse numbers similar to that seen in models of epilepsy (29,30).

Alternatively, in a second model, it is possible that depolarizing $GABA_A$ transmission provides shunting inhibition throughout the postnatal period, thereby restraining synapse formation and circuit activity during development (S5B-C Fig, green shaded area). Indeed, emerging evidence suggests that depolarizing $GABA_A$ transmission exerts inhibitory effects on ENOs *in vivo*, from at least P3 onward (Kirmse et al., 2015; Valeeva et al., 2016; Che et al., 2018). Consistent with this, our results in slices cultured from younger mice (S1D-F Fig) suggest that $GABA_A$ transmission restrains synapse formation over a period of up to 5 days of hippocampal circuit development. While previous work has admittedly demonstrated that prematurely rendering $GABA_A$ transmission hyperpolarizing *in vivo* decreases glutamatergic synapse formation (Ge et al., 2006; Cancedda et al., 2007; Wang and Kriegstein, 2008, 2011), it is noteworthy that

these earlier studies manipulated E_{Cl} over extended periods that spanned multiple phases of postmitotic neuronal development, including cell migration, axonal/dendritic growth, synapse formation and circuit refinement. Depolarizing $GABA_A$ transmission is thought to play important roles in all of these processes (Owens and Kriegstein, 2002), and hence the observed effects of prematurely reducing E_{Cl} on synapses may be secondary to other alterations in neuronal and circuit development. Indeed, soma size and dendritic branching are altered when GABA is prematurely rendered hyperpolarizing over an extended time period (Cancedda et al., 2007; Wang and Kriegstein, 2008). More temporally precise manipulations of $GABA_A$ transmission and E_{Cl} are therefore essential for clarifying the roles of GABA during critical phases of synapse formation *in vivo*. Interestingly, the finding that propofol administered to postnatal day 10 rats decreased spine number supports the notion that there is a developmental period *in vivo* during which immature $GABA_A$ transmission restrains glutamatergic synapse formation (Puskarjov et al., 2017).

When considering these two models, it is important to note that an inhibitory effect of depolarizing $GABA_A$ transmission does not preclude a role for GABA in driving ENOs, as it has been demonstrated that depolarizing chloride currents are only involved in the initial generation of GDPs in acute slices, after which they inhibit the continuation of the same GDPs (Khalilov et al., 2015). Thus, depolarizing $GABA_A$ transmission may simultaneously generate ENOs, while also maintaining control of wider circuit activity, thereby limiting runaway glutamatergic synapse formation. These dichotomous effects of GABA may rely on where GABAergic inputs impinge on the post synaptic neuron. Gulledge and Steward (2003) showed that in young rats, puffing GABA on distal dendrites of Layer 5 pyramidal cells facilitated firing, while puffing GABA on the cell body inhibited firing. Thus, different GABAergic interneuron subtypes may be responsible for driving ENOs vs restraining glutamatergic synapse formation. Furthermore, despite the evidence suggesting GABA is inhibitory throughout most of postnatal development *in vivo*, it has been shown that high frequency uncaging or stimulated release of GABA onto dendrites of layer 2/3 pyramidal cells in the neocortex can elicit formation of glutamatergic and GABAergic synapses during development *in vivo* (Oh et al., 2016). Although it remains to be seen whether endogenous patterns of GABA release can have similar effects, it

appears there may be a local trophic role for depolarizing $GABA_A$ transmission, which may promote synapse formation even as its circuit-wide inhibitory effects restrain the same process as we have demonstrated. More work is needed to dissect the possible roles of GABA in local synapse formation and more global circuit development, and to understand how the role of GABA changes across development.

Sustained Changes in Glutamatergic Synapses and Neurodevelopmental Disorders

Remarkably, we found that a transient blockade of depolarizing, inhibitory $GABA_A$ transmission led to a sustained increase in both the number of glutamatergic synapses and the proportion of thin spines, indicating that transient manipulations of immature $GABA_A$ transmission can profoundly alter hippocampal connectivity (Fig 4). Using slice cultures allowed for more temporally precise manipulations that revealed this effect, though it remains to be seen if the phenomenon persists *in vivo.* These questions are clinically relevant, as a role for GABA in restraining synapse formation may change how we understand and mitigate the effects of anticonvulsants, anaesthetics and drugs of abuse on neonatal, as well as fetal development, as GABA is believed to be depolarizing mainly in late gestation in humans (Vanhatalo et al., 2005; Sedmak et al., 2015). Furthermore, both the persistent increase in synapses and spines and the shift in spine morphologies we observed after recovery from transient GBZ treatment are reminiscent of “spinopathies” seen in intellectual disabilities including Fragile X syndrome and autism spectrum disorders (Lacey and Terplan, 1987; Irwin et al., 2000, 2001; Kaufmann and Moser, 2000; Fiala et al., 2002; Hutsler and Zhang, 2010). Numerous models of ASDs are associated with a delay in the depolarizing to hyperpolarizing shift in E_{GABA} (He et al., 2014; Tyzio et al., 2014; Leonzino et al., 2016). Such a delayed transition to hyperpolarizing E_{GABA} likely translates to a delay in the onset of adequate shunting inhibition when GABA is still depolarizing, which may increase glutamatergic synapse formation in a manner similar to that which we observed when blocking depolarizing/inhibitory $GABA_A$ transmission. Furthermore, mutation of the β3 $GABA_A$ receptor subunit, the expression of which peaks during development when GABA is depolarizing, has been observed in ASD (Menold et al., 2001; Buxbaum et al., 2002; Chen et al., 2014). The findings presented in the current study may provide a causal link

between these mutations and the hyperconnectivity observed in ASDs. Thus, further investigation is required to understand if impairments of depolarizing/inhibitory $GABA_A$ transmission contribute to the lasting alterations of spines and synapses in these conditions. Finally, the possibility that GABA bidirectionally controls synapse formation may yield novel clinical approaches for correcting synaptic deficits in neurodevelopmental disorders.

MATERIALS AND METHODS

Animals

Experiments were approved by the Montreal General Hospital Facility Animal Care Committee and followed guidelines of the Canadian Council on Animal Care. Male and female C57BL6 mice kept on a 12:12 light-dark cycle were used to prepare organoptypic cultures.

Slice Preparation

Organotypic hippocampal slices were prepared as described previously (Haber et al., 2006). Briefly, hippocampi were extracted from postnatal day 5 mice and cut into 300µm slices with a McIllwain tissue chopper (Stoelting). Slices were cultured on semiporous tissue culture inserts (Millipore) that sat in culture medium composed of minimal essential medium (MEM) supplemented with Glutamax (Invitrogen, Cat. No. 42360032), 25% horse serum (Invitrogen, Cat. No. 26050088), 25% HBSS (Invitrogen, Cat. No. 14025092), 6.5 mg/mL D-glucose and 0.5% penicillin/streptomycin. Slices were cultured for 5-14 days with full medium changes every 2 days.

Labeling of CA1 Cells

Dendrites and spines of CA1 pyramidal cells were labelled using a Semliki Forest Virus (SFV)-mediated approach describe in detail elsewhere (Haber et al., 2006). Briefly, SFV driving expression of enhanced green fluorescent protein, targeted to the cell membrane through a farnesylation sequence (EGFPf), was injected into the stratum oriens via pulled glass pipette, broken to a diameter of approximately 50 to 100 µm. Glass pipettes were attached to a Picospritzer III (Parker Hannifin) and SFV was delivered with 10ms pulses

at 14 to 18 psi 18 to 20 hours before fixation in 4% formaldehyde/0.1 M PO_4^{2-} for 30 min.

Confocal Imaging and Spine Analysis

Imaging was performed using an Ultraview Spinning Disc confocal system (Perkin Elmer) attached to a Nikon TE-2000 microscope and a FV1000 laser scanning confocal microscope (Olympus). Z-stacks were acquired from approximately 100µm of CA1 primary apical dendrites, just above the primary dendrite bifurcation. This dendritic subfield is consistently identifiable, fully formed by the period of interest, harbors the highest density of asymmetric synapses, and retains its native connectivity in organotypic slices (Megias et al., 2001; Amaral and Lavenex, 2007). Ten to forty z-stacks were acquired per animal (2-4 animals per experiment, minimum 3 experiments per dataset). Two-dimensional spine counts and geometric measurements of spines were quantified using Reconstruct (Fiala, 2005) and a custom ImageJ macro. 3D spine classification was performed with NeuronStudio (Rodriguez et al., 2008). All spine analysis was performed by an investigator blinded to the experimental condition.

Western Blot Analysis

For Western blots, 4-6 organotypic slices were lifted from nylon culture inserts with a No. 10 scalpel blade, rinsed in cold PBS and incubated on ice in 100µL of Triton lysis buffer (20 mM Tris pH7.4, 137 mM NaCl, 2mM EDTA, 1% Triton X-100 (TX-100), 0.1% SDS, 10% glycerol, with protease inhibitors and sodium orthovanadate) for 30 min. Lysates were centrifuged at high speed for 10 min and stored at -80°C in sample buffer. Supernatants were warmed to room temperature and run under standard SDS-PAGE conditions. Membranes were immunoblotted with anti-KCC2 1:1000 (N1/12, NeuroMab, CA) and GAPDH 1:300,000 (MAB374, Millipore). KCC2 blots were run immediately after developmental time courses ended to reduce experimentally-induced aggregation of KCC2 oligomers, which we observe to increase with time at -80°C.

Electrophysiology

Gramicidin perforated patch whole cell recordings were performed similar to previously described (Acton et al., 2012). Briefly, current-voltage (IV) curves were generated by step depolarizing the membrane potential in 10mV increments from ~-95 to -35mV (Fig 1C) and during each increment GABAergic transmission was elicited via extracellular

stimulation in the stratum radiatum. Pipettes had a resistance of 7–12 MΩ and were filled with an internal solution containing 150mM KCl, 10mM HEPES, and 50mM µg/ml gramicidin (pH 7.4, 300 mOsm). We recorded E_{GABA} in current clamp mode. Glutamatergic transmission was inhibited with CNQX.

Miniature EPSCs (mEPSCs) were recorded using the whole-cell patch clamp configuration (V_h = -70mV), at 30°C, in ACSF containing (in mM): 119 NaCl, 26.2 $NaHCO_3$, 11 D-glucose, 2.5 KCl, 1 NaH_2PO_4, 2.5 $CaCl_2$, 1.3 $MgCl_2$, 0.0002 TTX, 0.025 D-APV, 0.05 picrotoxin. Recording pipettes (2-5 MΩ) were filled with (in mM): 122 $CsMeSO_4$, 8 NaCl, 10 D-glucose, 1 $CaCl_2$, 10 EGTA, 10 HEPES, 0.3 Na_3GTP, 2 MgATP, pH 7.2. Signals were low-pass filtered at 2kHz, acquired at 10 kHz, and analyzed using Clampfit 10.3 (Molecular Devices).

For cell attached recordings, ACSF and pipette solutions were as described above for mEPSC recordings, but ACSF lacked TTX, D-APV and picrotoxin. Low resistance recording pipettes (1-2 MΩ) were used to form loose patch seals (approximately 100-350 MΩ). Recordings were performed in I=0 mode. GABA was diluted in ACSF to 100 µM and puffed in close proximity to the recorded cell using a glass pipette connected to a Picospritzer III (Parker Hannifin) delivering 10 ms duration air puffs at 14 psi. Electrically-evoked stimulations (1.3 V, 0.5 ms) were delivered by the recording amplifier via the recording pipette. Recorded signals were analyzed using threshold-based detection of spikes in Clampfit 10.3 (Molecular Devices).

Experiments comprised slices from at least 3 separate animals taken from at least 2 litters.

Pharmacology

Pharmacological agents (Tocris unless otherwise noted) were applied to the culture medium during a regular medium change. Gabazine (GBZ) (20µM), bicuculline-methiodide (20µM) and muscimol (10µM) were used to manipulate $GABA_A$ transmission. GBZ was washed out by incubating slices in fresh medium for 30 minutes, then washing the top of the slices with equilibrated medium for 1-2 minutes before changing to fresh dishes and medium. Bumetanide (Bume, 10 µM), TrkB-Fc bodies (5mg/mL, R&D Systems) and K252a (200 nM) were added to cultures 30 minutes before adding GBZ.

Quantitative Reverse Transcriptase PCR (qRT-PCR)

Six to eight organotypic slices per sample were lifted from nylon culture inserts with a No. 10 scalpel blade, washed briefly in ice cold PBS and flash frozen in microcentrifuge tubes in a 100% EtOH/dry ice slurry. Total RNA was extracted using the RNeasy Lipid Tissue Kit (Qiagen). cDNA libraries were created using QuantiTect Reverse Transcription Kit (Qiagen). Quantitative PCR was performed using Sybr Green Master Mix (Applied Biosystems Systems) on a StepOne Plus thermocycler (Applied Biosystems). Relative levels of mRNA were calculated using the ΔΔCT method with GAPDH as the internal control. Primer sequences were as follows: GAPDH forward TTG AAG TCG CAG GAG ACA ACC; GAPDH reverse ATG TGT CCG TCG TGG ATC; BDNF forward GTG ACA GTA TTA GCG AGT GGG; BDNF reverse GGG ATT ACA CTT GGT CTC GTA G; Fos forward TCC CCA AAC TTC GAC CAT G; Fos reverse CAT GCT GGA GAA GGA GTC G.

Immunofluorescence

Slice cultures were fixed as described above, permeabilized for 30 minutes in 1% TritonX 100/PBS, blocked in 10% normal donkey serum (NDS, Jackson Immuno Research)/ 0.2% TX-100/PBS, and incubated with anti-c-Fos antibody (1:5000, Cat. No. 226 003, Synaptic Systems) in 1% NDS/0.2% TX-100/PBS rocking at 4°C for 5 days. Primary antibody solution was washed with 3 rinses in 1% NDS/0.2% TX-100/PBS, followed by secondary antibodies at 1:1000 for 2 hours at room temp. TOPRO-3-iodide (Jackson Immuno Research) was applied at 1:10,000 for 10 minutes in the second of three washes following incubation with secondary antibodies. Quantification of fluorescence intensity with background correction was performed with ImageJ, using mean pixel values in ROIs traced manually around cell bodies.

Statistics

Data is presented as mean ± SEM. Student t-tests were used except where noted that Mann-Whitney tests were used with datasets with non-normal distribution. Post hoc pairwise comparisons following ANOVA were performed with Tukey's honestly significant

difference (HSD) test. For mean comparisons: *p<0.05, **p<0.01, ***p<0.001. For Kolmogorov-Smirnov tests: ***p<0.0001.

REFERENCES

Acton BA, Mahadevan V, Mercado A, Uvarov P, Ding Y, Pressey J, Airaksinen MS, Mount DB, Woodin MA (2012) Hyperpolarizing GABAergic transmission requires the KCC2 C-terminal ISO domain. J Neurosci 32:8746–8751.

Akerman CJ, Cline HT (2006) Depolarizing GABAergic conductances regulate the balance of excitation to inhibition in the developing retinotectal circuit in vivo. J Neurosci 26:5117–5130.

Akerman CJ, Cline HT (2007) Refining the roles of GABAergic signaling during neural circuit formation. Trends Neurosci 30:382–389.

Amaral D, Lavenex P (2007) The Hippocampus Book (Andersen P, Morris R, Amaral D, Bliss T, O'Keefe J, eds). Oxford: Oxford University Press.

Balkowiec A, Katz DM (2002) Cellular mechanisms regulating activity-dependent release of native brain-derived neurotrophic factor from hippocampal neurons. J Neurosci 22:10399–10407.

Behar TN, Schaffner AE, Scott CA, Greene CL, Barker JL (2000) GABA receptor antagonists modulate postmitotic cell migration in slice cultures of embryonic rat cortex. Cereb Cortex 10:899–909.

Ben-Ari Y (2002) Excitatory actions of GABA during development: the nature of the nurture. Nat Rev Neurosci 3:728–739.

Ben-Ari Y, Cherubini E, Corradetti R, Gaiarsa J (1989) Giant synaptic potentials in immature rat CA3 hippocampal neurones. J Physiol 416:303–325.

Ben-Ari Y, Gaiarsa J-L, Tyzio R, Khazipov R (2007) GABA: a pioneer transmitter that excites immature neurons and generates primitive oscillations. Physiol Rev 87:1215–1284.

Ben-ari Y, Khazipov R, Leinekugel X, Caillard O, Gaiarsa J (1997) GABAA, NMDA and AMPA receptors : a developmentally regulated 'ménage à trois.' Trends Neurosci 20:523–529.

Ben-Ari Y, Woodin MA, Sernagor E, Cancedda L, Vinay L, Rivera C, Legendre P,

596 Luhmann HJ, Bordey A, Wenner P, Fukuda A, van den Pol AN, Gaiarsa J-L,
597 Cherubini E (2012) Refuting the challenges of the developmental shift of polarity of
598 GABA actions: GABA more exciting than ever! Front Cell Neurosci 6:35.

599 Buchs P-A, Stoppini L, Muller D (1993) Structural modifications associated with synaptic
600 development in area CA1 of rat hippocampal organotypic cultures. Brain Res Dev
601 Brain Res 71:81–91.

602 Buxbaum JD, Silverman JM, Smith CJ, Greenberg D a, Kilifarski M, Reichert J, Cook
603 EH, Fang Y, Song C-Y, Vitale R (2002) Association between a GABRB3
604 polymorphism and autism. Mol Psychiatry 7:311–316.

605 Cancedda L, Fiumelli H, Chen K, Poo M (2007) Excitatory GABA action is essential for
606 morphological maturation of cortical neurons in vivo. J Neurosci 27:5224–5235.

607 Chancey JH, Adlaf EW, Sapp MC, Pugh PC, Wadiche JI, Overstreet-Wadiche LS
608 (2013) GABA depolarization is required for experience-dependent synapse
609 unsilencing in adult-born neurons. J Neurosci 33:6614–6622.

610 Chapleau C a, Larimore JL, Theibert A, Pozzo-Miller L (2009) Modulation of dendritic
611 spine development and plasticity by BDNF and vesicular trafficking: fundamental
612 roles in neurodevelopmental disorders associated with mental retardation and
613 autism. J Neurodev Disord 1:185–196.

614 Che A, Babij R, Iannone AF, Liston C, Fishell G, De Marco Garcia N V (2018) Layer I
615 Interneurons Sharpen Sensory Maps during Neonatal Development. Neuron
616 99:98–116.

617 Chen C-H, Huang C-C, Cheng M-C, Chiu Y-N, Tsai W-C, Wu Y-Y, Liu S-K, Gau SS-F
618 (2014) Genetic analysis of GABRB3 as a candidate gene of autism spectrum
619 disorders. Mol Autism 5:36.

620 De Simoni A, Griesinger CB, Edwards FA (2003) Development of rat CA1 neurones in
621 acute versus organotypic slices: role of experience in synaptic morphology and
622 activity. J Physiol 550:135–147.

623 Drakew A, Muller M, Gahwiler B, Thompson S, Frotscher M (1996) Spine Loss in
624 Experimental Epilepsy: Quantitative Light and Electron Miscroscopic Analysis of

625 Intracellularly Stained CA3 Pyramidal Cells in Hippocampal Slice Cultures.
626 Neuroscience 70:31–45.

627 Dzhala VI, Talos DM, Sdrulla DA, Brumback AC, Mathews GC, Benke TA, Delpire E,
628 Jensen FE, Staley KJ (2005) NKCC1 transporter facilitates seizures in the
629 developing brain. Nat Med 11:1205–1213.

630 El Marroun H, White T, Verhulst FC, Tiemeier H (2014) Maternal use of antidepressant
631 or anxiolytic medication during pregnancy and childhood neurodevelopmental
632 outcomes: a systematic review. Eur Child Adolesc Psychiatry 23:973–992.

633 Fiala JC (2005) Reconstruct : a free editor for serial section microscopy. J Microsc
634 218:52–61.

635 Fiala JC, Spacek J, Harris KM (2002) Dendritic Spine Pathology : Cause or
636 Consequence of Neurological Disorders ? Brain Res Rev 39:29–54.

637 Fiumelli H, Briner A, Puskarjov M, Blaesse P, Belem BJ, Dayer AG, Kaila K, Martin J-L,
638 Vutskits L (2012) An Ion Transport-Independent Role for the Cation-Chloride
639 Cotransporter KCC2 in Dendritic Spinogenesis In Vivo. Cereb Cortex.

640 Garaschuk O, Hanse E, Konnerth A (1998) Developmental profile and synaptic origin of
641 early network oscillations in the CA1 region of rat neonatal hippocampus. J Physiol
642 507 (Pt 1:219–236.

643 Ge S, Goh ELK, Sailor K a, Kitabatake Y, Ming G, Song H (2006) GABA regulates
644 synaptic integration of newly generated neurons in the adult brain. Nature 439:589–
645 593.

646 Griguoli M, Cherubini E (2017) Early Correlated Network Activity in the Hippocampus :
647 Its Putative Role in Shaping Neuronal Circuits. Front Cell Neurosci 11:1–11.

648 Gulledge AT, Stuart GJ (2003) Excitatory actions of GABA in the cortex. Neuron
649 37:299–309.

650 Haber M, Zhou L, Murai KK (2006) Cooperative Astrocyte and Dendritic Spine
651 Dynamics at Hippocampal Excitatory Synapses. 26:8881–8891.

652 Hanse E, Durand GM, Garaschuk O, Konnerth A (1997) Activity-dependent wiring of the

653 developing hippocampal neuronal circuit. Semin Cell Dev Biol 8:35–42.

654 He Q, Nomura T, Xu J, Contractor A (2014) The Developmental Switch in GABA
655 Polarity Is Delayed in Fragile X Mice. J Neurosci 34:446–450.

656 Heaulme M, Chambon JP, Leyris R, Molimard JC, Wermuth CG, Biziere K (1986)
657 Biochemical characterization of the interaction of three pyridazinyl-GABA
658 derivatives with the $GABA_A$ receptor site. Brain Res 384:224–231.

659 Heck N, Kilb W, Reiprich P, Kubota H, Furukawa T, Fukuda A, Luhmann HJ (2007)
660 GABA-A receptors regulate neocortical neuronal migration in vitro and in vivo.
661 Cereb Cortex 17:138–148.

662 Hutsler JJ, Zhang H (2010) Increased dendritic spine densities on cortical projection
663 neurons in autism spectrum disorders. Brain Res 1309:83–94.

664 Irwin SA, Galvez R, William T (2000) Dendritic Spine Structural Anomalies in Fragile-X
665 Mental Retardation Syndrome. :1038–1044.

666 Irwin SA, Patel B, Idupulapati M, Harris JB, Crisostomo RA, Larsen BP, Kooy F,
667 Willems PJ, Cras P, Kozlowski PB, Swain RA, Weiler IJ, Greenough WT (2001)
668 Abnormal dendritic spine characteristics in the temporal and visual cortices of
669 patients with fragile-X syndrome: a quantitative examination. Am J Med Genet
670 98:161–167.

671 Ji Y, Lu Y, Yang F, Shen W, Tang TTT, Feng L, Duan S, Lu B (2010) Acute and gradual
672 increases in BDNF concentration elicit distinct signaling and functions in neurons.
673 Nat Neurosci 13:302–309.

674 Johnston GAR (2014) Muscimol as an Ionotropic GABA Receptor Agonist. Neurochem
675 Res 39:1942–1947.

676 Jourdain P, Nikonenko I, Alberi S, Muller D (2002) Remodeling of Hippocampal
677 Synaptic Networks by a Brief Anoxia – Hypoglycemia. 22:3108–3116.

678 Kaila K (1994) Ionic Basis of GABAA Receptor Channel Function in the Nervous
679 System. Prog Neurobiol 42:489–437.

680 Kaufmann WE, Moser HW (2000) Dendritic Anomalies in Disorders Associated with

681 Mental Retardation. :981–991.

682 Khalilov I, Dzhala V, Ben-Ari Y, Khazipov R (1999) Dual Role of GABA in the Neonatal
683 Rat Hippocampus. Dev Neurosci 21:310–319.

684 Khalilov I, Minlebaev M, Mukhtarov M, Khazipov R (2015) Dynamic Changes from
685 Depolarizing to Hyperpolarizing GABAergic Actions during Giant Depolarizing
686 Potentials in the Neonatal Rat Hippocampus. 35:12635–12642.

687 Khazipov R, Leinekugel X, Khalilov I, Gaiarsa J, Ben-ari Y (1997) Synchronization of
688 GABAergic interneuronal network in CA3 subfield of neonatal rat hippocampal
689 slices. J Physiol 483:763–772.

690 Kirmse K, Hübner CA, Isbrandt D, Witte OW (2018) GABAergic Transmission during
691 Brain Development: Multiple Effects at Multiple Stages. Neurosci 24:36–53.

692 Kirmse K, Kummer M, Kovalchuk Y, Witte OW, Garaschuk O, Holthoff K (2015) GABA
693 depolarizes immature neurons and inhibits network activity in the neonatal
694 neocortex in vivo. Nat Commun 6.

695 Lacey DJ, Terplan K (1987) Abnormal Cerebral Cortical Neurons in a Child With
696 Maternal PKU Syndrome. J Child Neurol 2:201–204.

697 Lamsa KP, Palva JM, Ruusuvuori E, Kaila K, Taira T (2000) Synaptic GABA A
698 Activation Inhibits AMPA-Kainate Receptor – Mediated Bursting in the Newborn (
699 P0 – P2) Rat Hippocampus. J Neurophysiol 83:359–366.

700 Le Magueresse C, Safiulina V, Changeux J-P, Cherubini E (2006) Nicotinic modulation
701 of network and synaptic transmission in the immature hippocampus investigated
702 with genetically modified mice. J Physiol 576:533–546.

703 Leinekugel X, Tseeb V, Ben-ari Y, Bregestovski P (1995) Synaptic GABAA activation
704 induces Ca2+ rise in pyramidal cells and interneurons from rat neonatal
705 hippocampal slices. J Physiol 487:319–329.

706 Leonzino M, Busnelli M, Antonucci F, Verderio C, Mazzanti M, Chini B, Leonzino M,
707 Busnelli M, Antonucci F, Verderio C, Mazzanti M, Chini B (2016) The Timing of the
708 Excitatory-to-Inhibitory GABA Switch Is Regulated by the Oxytocin Receptor Report
709 The Timing of the Excitatory-to-Inhibitory GABA Switch Is Regulated by the

710 Oxytocin Receptor via KCC2. :96–103.

711 Li H, Khirug S, Cai C, Ludwig A, Blaesse P, Kolikova J, Afzalov R, Coleman SK, Lauri
712 S, Airaksinen MS, Keinänen K, Khiroug L, Saarma M, Kaila K, Rivera C (2007)
713 KCC2 interacts with the dendritic cytoskeleton to promote spine development.
714 Neuron 56:1019–1033.

715 Liu X, Wang Q, Haydar TF, Bordey A (2005) Nonsynaptic GABA signaling in postnatal
716 subventricular zone controls proliferation of GFAP-expressing progenitors. Nat
717 Neurosci 8:1179–1187.

718 Megias M, Emri Z, Gulyas A, Freund T (2001) Total number and distribution of inhibitory
719 and excitatory synapses on hippocampal CA1 pyramidal cells. Neuroscience
720 102:527–540.

721 Menold MM, Shao Y, Wolpert CM, Donnelly SL, Raiford KL, Martin ER, Ravan S a,
722 Abramson RK, Wright HH, Delong GR, Cuccaro ML, Pericak-Vance M a, Gilbert JR
723 (2001) Association analysis of chromosome 15 gabaa receptor subunit genes in
724 autistic disorder. J Neurogenet 15:245–259.

725 Mohajerani MH, Cherubini E (2005) Spontaneous recurrent network activity in
726 organotypic rat hippocampal slices. Eur J Neurosci 22:107–118.

727 Mortensen M, Ebert B, Wafford K, Smart TG (2010) Distinct activities of GABA agonists
728 at synaptic- and extrasynaptic-type GABAA receptors. J Physiol 588:1251–1268.

729 Muller D, Buchs P-A, Stoppini L (1993) Time course of synaptic development in
730 hippocampal organotypic cultures. Brain Res Dev Brain Res 71:93–100.

731 Oh WC, Lutzu S, Castillo PE, Kwon HB (2016) De novo synaptogenesis induced by
732 GABA in the developing mouse cortex. Science (80-) 353.

733 Owens DF, Kriegstein AR (2002) Is there more to GABA than synaptic inhibition? Nat
734 Rev Neurosci 3:715–727.

735 Park H, Poo MM (2013) Neurotrophin regulation of neural circuit development and
736 function. Nat Rev Neurosci 14:7–23.

737 Pérez-Gómez A, Tasker RA (2013) Transient domoic acid excitotoxicity increases

738 BDNF expression and activates both MEK- and PKA-dependent neurogenesis in
739 organotypic hippocampal slices. BMC Neurosci 14:72.

740 Puskarjov M, Ahmad F, Khirug S, Sivakumaran S, Kaila K, Blaesse P (2014) BDNF is
741 required for seizure-induced but not developmental up-regulation of KCC2 in the
742 neonatal hippocampus. Neuropharmacology 88:1–7.

743 Puskarjov M, Fiumelli H, Briner A, Bodogan T, Demeter K, Lacoh C, Mavrovic M,
744 Blaesse P, Kaila K, Vutskits L (2017) K-Cl Cotransporter 2-mediated Cl- extrusion
745 determine developmental stage-dependent impact of propofol mediated anesthesia
746 on dendritic spines. Anesthesiology 126:1–13.

747 Rivera C, Voipio J, Payne JA (1999) The K+/Cl- co-transporter KCC2 renders GABA
748 hyperpolarizing during neuronal maturation. Nature 397:251–255.

749 Rodriguez A, Ehlenberger DB, Dickstein DL, Hof PR, Wearne SL (2008) Automated
750 three-dimensional detection and shape classification of dendritic spines from
751 fluorescence microscopy images. PLoS One 3.

752 Sedmak G, Jovanov-Milošević N, Puskarjov M, Ulamec M, Krušlin B, Kaila K, Judaš M
753 (2015) Developmental Expression Patterns of KCC2 and Functionally Associated
754 Molecules in the Human Brain. Cereb Cortex:1–16.

755 Sokal DM, Mason R, Parker TL (2000) Multi-neuronal recordings reveal a differential
756 effect of thapsigargin on bicuculline- or gabazine-induced epileptiform excitability in
757 rat hippocampal neuronal networks. Neuropharmacology 39:2408–2417.

758 Staley KJ, Mody I (1992) Shunting of excitatory input to dentate gyrus granule cells by a
759 depolarizing GABAA receptor-mediated postsynaptic conductance. J Neurophysiol
760 68:197–212.

761 Staley KJ, Proctor WR (1999) Modulation of mammalian dendritic GABAA receptor
762 function by the kinetics of Cl- and HCO3- transport. J Physiol 519:693–712.

763 Swann JW, Brady RJ, Martin DL (1989) Postnatal development of GABA-mediated
764 synaptic inhibition in rat hippocampus. Neuroscience 28:551–561.

765 Tyler WJ, Pozzo-Miller L (2003) Miniature synaptic transmission and BDNF modulate
766 dendritic spine growth and form in rat CA1 neurones. J Physiol 553:497–509.

767 Tyzio R, Nardou R, Ferrari DC, Tsintsadze T, Shahrokhi A, Eftekhari S, Khalilov I,
768 Tsintsadze V, Brouchoud C, Chazal G, Lemonnier E, Lozovaya N, Burnashev N,
769 Ben-Ari Y (2014) Oxytocin-Mediated GABA Inhibition During Delivery Attenuates
770 Autism Pathogenesis in Rodent Offspring. Science (80-) 343:675–680.

771 Valeeva G, Tressard T, Mukhtarov M, Baude A, Khazipov R (2016) An Optogenetic
772 Approach for Investigation of Excitatory and Inhibitory Network GABA Actions in
773 Mice Expressing Channelrhodopsin-2 in GABAergic Neurons. J Neurosci 36:5961–
774 5973.

775 Vanhatalo S, Palva JM, Andersson S, Rivera C, Voipio J, Kaila K (2005) Slow
776 endogenous activity transients and developmental expression of K+-Cl-
777 cotransporter 2 in the immature human cortex. Eur J Neurosci 22:2799–2804.

778 Vicario-Abejón C, Collin C, McKay RD, Segal M (1998) Neurotrophins induce formation
779 of functional excitatory and inhibitory synapses between cultured hippocampal
780 neurons. J Neurosci 18:7256–7271.

781 Vicario-Abejón C, Owens D, McKay R, Segal M (2002) Role of neurotrophins in central
782 synapse formation and stabilization. Nat Rev Neurosci 3:965–974.

783 Wang DD, Kriegstein AR (2008) GABA regulates excitatory synapse formation in the
784 neocortex via NMDA receptor activation. J Neurosci 28:5547–5558.

785 Wang DD, Kriegstein AR (2009) Defining the role of GABA in cortical development. J
786 Physiol 587:1873–1879.

787 Wang DD, Kriegstein AR (2011) Blocking early GABA depolarization with bumetanide
788 results in permanent alterations in cortical circuits and sensorimotor gating deficits.
789 Cereb Cortex 21:574–587.

790 Wells JE, Porter JT, Agmon A, Virginia W (2000) GABAergic Inhibition Suppresses
791 Paroxysmal Network Activity in the Neonatal Rodent Hippocampus and Neocortex.
792 J Neurosci 20:8822–8830.

793 Yamada J, Okabe A, Toyoda H, Kilb W, Luhmann HJ, Fukuda A (2004) Cl- uptake
794 promoting depolarizing GABA actions in immature rat neocortical neurones is
795 mediated by NKCC1. J Physiol 557:829–841.

796 Zeng L, Xu L, Rensing NR, Sinatra PM, Rothman SM, Wong M (2007) Kainate Seizures
797 Cause Acute Dendritic Injury and Actin Depolymerization In Vivo. J Neurosci
798 27:11604–11613.

799 Zha X-M, Green SH, Dailey ME (2005) Regulation of hippocampal synapse remodeling
800 by epileptiform activity. Mol Cell Neurosci 29:494–506.

801

802

803

804

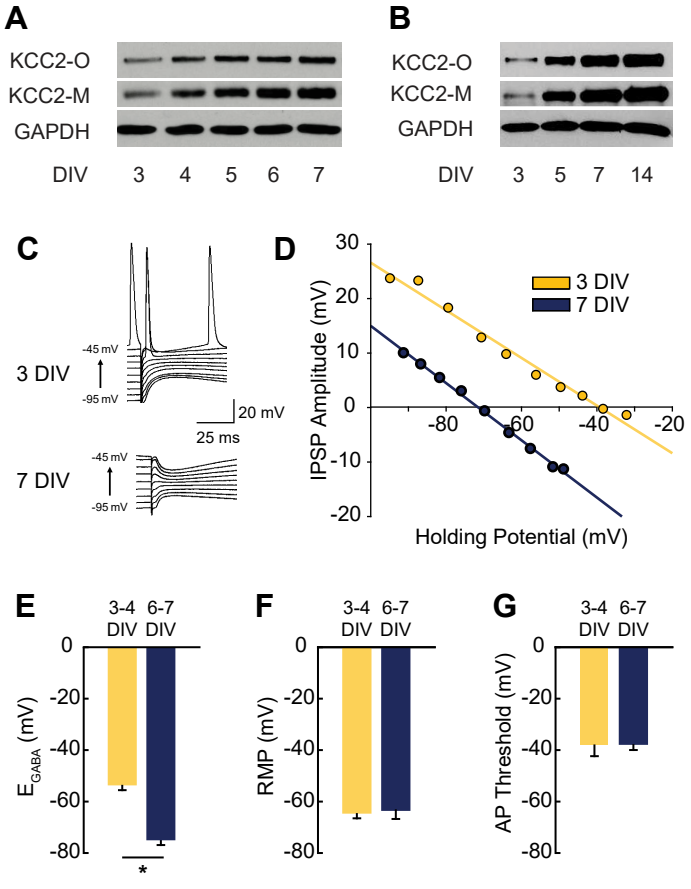
A
KCC2-O
KCC2-M
GAPDH
DIV 3 4 5 6 7
B
KCC2-O
KCC2-M
GAPDH
DIV 3 5 7 14
C
3 DIV
-45 mV
-95 mV
20 mV
25 ms
7 DIV
-45 mV
-95 mV
D
3 DIV
7 DIV
IPSP Amplitude (mV)
30
20
10
0
-10
-20
-80
-60
-40
-20
Holding Potential (mV)
E
3-4 DIV
6-7 DIV
E_{GABA} (mV)
0
-20
-40
-60
-80
*
F
3-4 DIV
6-7 DIV
RMP (mV)
0
-20
-40
-60
-80
G
3-4 DIV
6-7 DIV
AP Threshold (mV)
0
-20
-40
-60
-80

Figure 1

Figure 1. GABA reversal potential (E_{GABA}) shifts from depolarizing to hyperpolarizing between 3 and 7 DIV. ***A-B***, High (A) and low (B) temporal resolution western blots showing increasing expression of KCC2 monomers (KCC2-M) and oligomers (KCC2-O). ***C-D****,* Representative traces and representative IV curves from GABAergic responses at 3DIV and 7DIV. ***E***, E_{GABA} summary plots (3/4 DIV: -53.3±6.1mV, n=5; 6/7 DIV: -74.7± 6.4mV, n=5, p=0.04). ***F,*** Resting membrane potential summary plots (3/4 DIV: -64.5±2.3mV, n=5; 6/7 DIV: -63.4 ± 3.8mV, n=5). ***G****,* Action potential threshold summary plot (3/4 DIV: -38.2 ± 4.2mV, n=5; 6/7 DIV-37.7 ± 2.3mV, n=5).

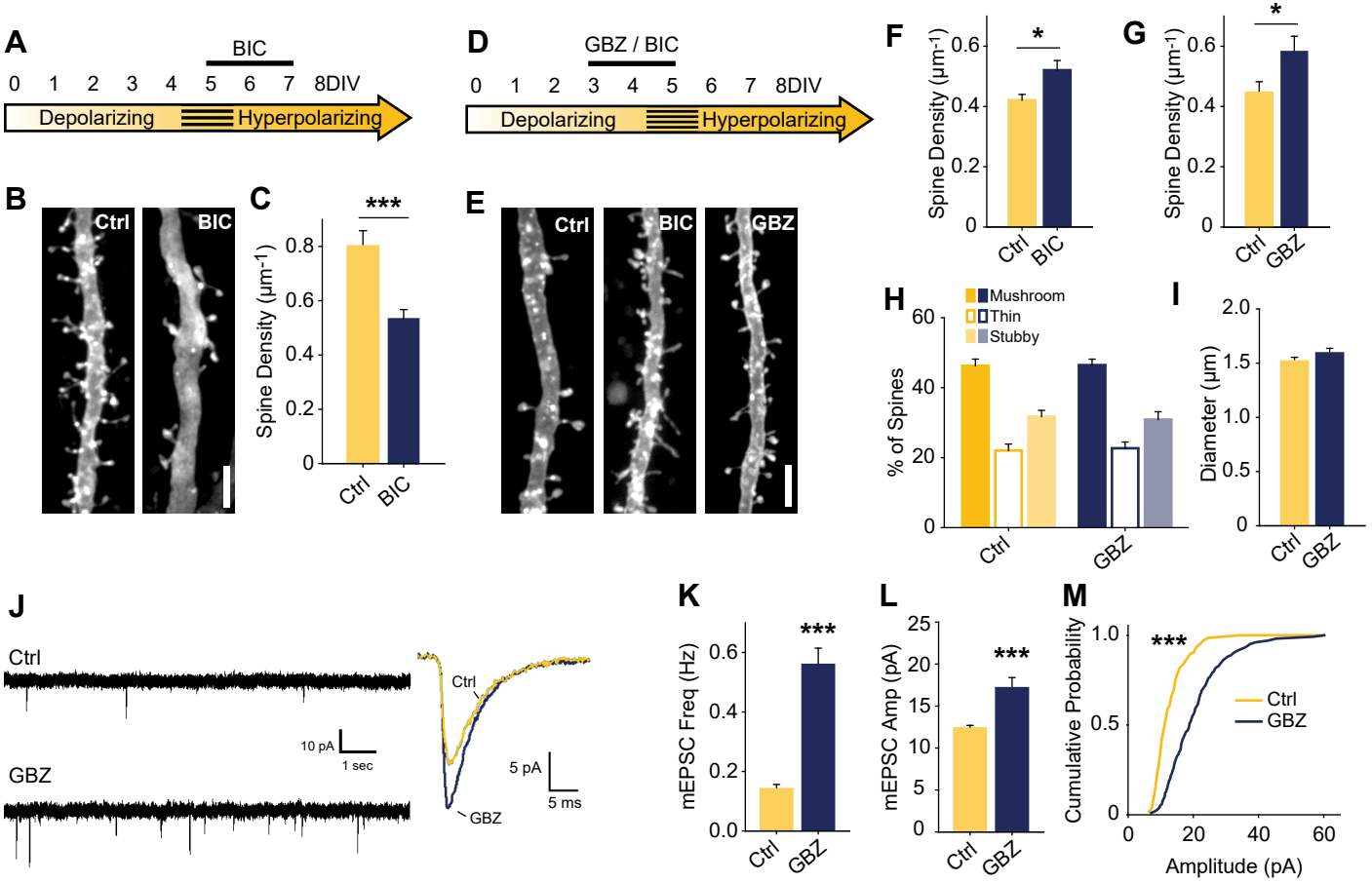
A
BIC
0 1 2 3 4 5 6 7 8DIV
Depolarizing
Hyperpolarizing
D
GBZ / BIC
0 1 2 3 4 5 6 7 8DIV
Depolarizing
Hyperpolarizing
B
Ctrl
BIC
C
***
Spine Density (µm-1)
Ctrl
BIC
E
Ctrl
BIC
GBZ
F
*
Spine Density (µm-1)
Ctrl
BIC
G
*
Spine Density (µm-1)
Ctrl
GBZ
H
Mushroom
Thin
Stubby
% of Spines
Ctrl
GBZ
I
Diameter (µm)
Ctrl
GBZ
J
Ctrl
10 pA
1 sec
GBZ
Ctrl
5 pA
5 ms
GBZ
K
***
mEPSC Freq (Hz)
Ctrl
GBZ
L
***
mEPSC Amp (pA)
Ctrl
GBZ
M
***
Cumulative Probability
Ctrl
GBZ
Amplitude (pA)

Figure 2

Figure 2. Blocking depolarizing $GABA_A$ transmission increases excitatory synapse number. ***A***, Time course of bicuculline (BIC) treatment for B-C. ***B-C****,* Spine density after 5-7 DIV BIC treatment (Control 0.80±0.06 spines/um, n=36, BIC 0.53±0.03, n=50; N=3; p<0.001, Mann-Whitney).***D****,* Time course of pharmacological treatments for E-M. ***E-G****,* Spine density after 3-5 DIV GBZ (G: Control 0.44±0.12 spines/um, n=145, GBZ 0.58±0.17, n=77; N=11; p=0.04) and BIC treatment (F: Control 0.42±0.02 spines/um, n=55, BIC 0.52±0.03 spines/um, n=41; N=9; P=0.027, Mann-Whitney). ***H,I****,* 3D spine morphology and dendrite diameter after GBZ. ***J****,* Representative traces of mEPSCs. ***K***, mEPSC frequency summary plot (Control 0.14±0.02 Hz, GBZ 0.56±0.06 Hz, p<0.001, Mann-Whitney). ***L****,* mEPSC amplitude summary plot (Control 12.32±0.37 pA, n=8, GBZ 17.12±1.27 pA, n=10, p<0.001, Mann-Whitney). ***M****,* Cumulative distributions of amplitudes (p<0.0001, Kolmogorov-Smirnov test). Scale bars 3μm.

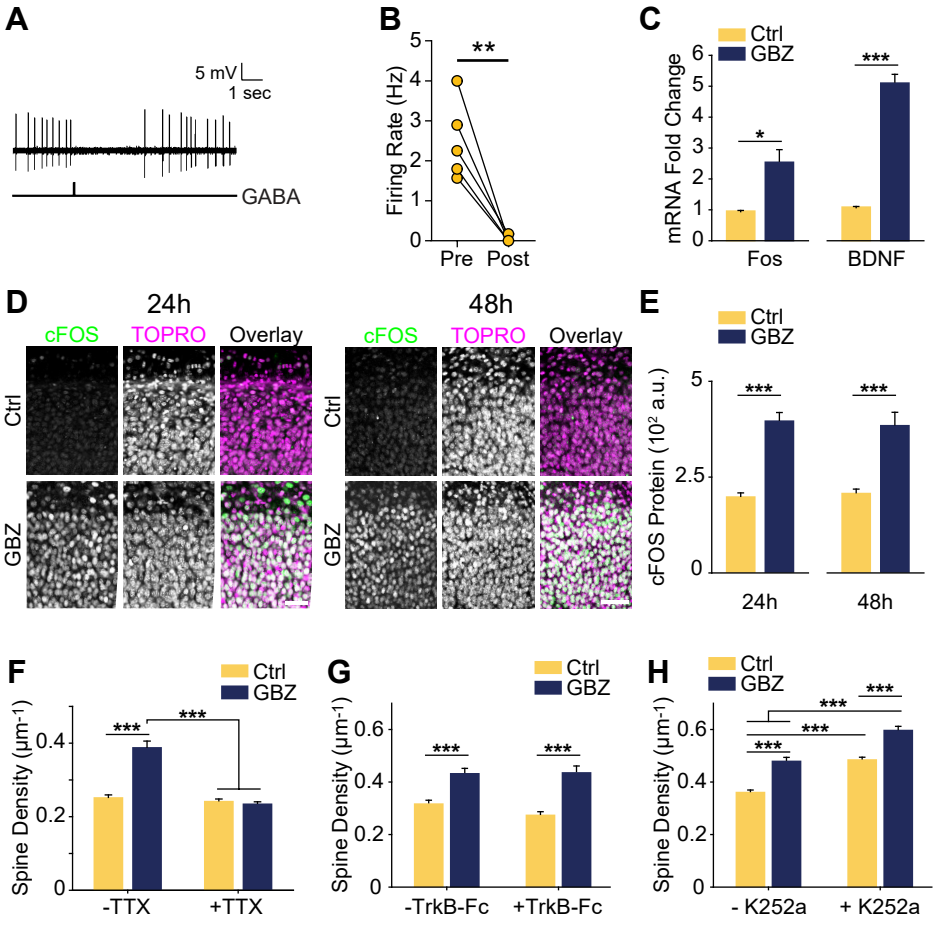
A
5 mV
1 sec
GABA
B
Firing Rate (Hz)
**
Pre
Post
C
Ctrl
GBZ
mRNA Fold Change
*
***
Fos
BDNF
D
24h
48h
cFOS
TOPRO
Overlay
Ctrl
GBZ
E
Ctrl
GBZ
cFOS Protein (10² a.u.)
***
24h
48h
F
Ctrl
GBZ
Spine Density (µm⁻¹)
***
-TTX
+TTX
G
Ctrl
GBZ
Spine Density (µm⁻¹)
***
-TrkB-Fc
+TrkB-Fc
H
Ctrl
GBZ
Spine Density (µm⁻¹)
***
- K252a
+ K252a

Figure 3

Figure 3. Increase in spine density following blockade of depolarizing/inhibitory $GABA_A$ transmission is activity-dependent but does not rely on BDNF signalling. . ***A,*** Sample trace of spontaneous activity inhibited by puffing on GABA. The line trace below indicates time of GABA puff. ***B,*** Summary plots of spontaneous activity pre- and post-GABA puff. ***C***, BDNF and Fos transcript levels following GBZ from 3-5DIV (BDNF: Ctrl 1.07±0.04, GBZ 5.08±0.3, N=3, p<0.001; Fos: Ctrl 0.94±0.04, GBZ 2.52±0.4, N=3, p=0.02). ***D,*** Fos immunofluorescence 24 and 48 hours after GBZ treatment at 3DIV. Images depict the dividing line between stratum oriens (upper portion of panels) and stratum pyramidale (lower portion of panels) in area CA1. TOPRO-3-Iodide was used to visualize nuclei. ***E***, Quantification of Fos immunofluorescence following 24h (Ctrl 196.5±12.2 au, n=10, GBZ 394.4±24.0 au, n=11, p<0.001) and 48h (Ctrl 205.6±12.1 au, n=10, GBZ 382.7±36.3 au, n=10, p<0.001, Mann-Whitney) of GBZ treatment which started at 3DIV. **F,** Quantification of spine density following GBZ and/or TTX treatment beginning at 3DIV (Ctrl 0.25±0.01 μm^{-1}, n= 196, GBZ 0.39±0.01 μm^{-1}, n=110, TTX 0.24±0.01 μm^{-1}, n= 166, GBZ+TTX 0.23±0.01μm^{-1}, n=154; N=5). Two-way ANOVA indicates a significant interaction between GBZ and TTX conditions, p<0.001. Significant differences between GBZ and all other conditions, p<0.001, Tukey post test. ***G***, Quantification of spine density following GBZ and/or TrkB-Fc treatment (Ctrl 0.31±0.02, n=86, GBZ 0.42±0.02, n=68, TrkB-Fc 0.27±0.02, n=96, TrkB-Fc+GBZ 0.43±0.02, n=61; N=3; 2 Way ANOVA, no interaction, Tukey post test). ***H***, Quantification of spine density following GBZ and/or K252a treatment (Ctrl 0.35±0.01, n=198, GBZ 0.49±0.03, n=144, K252a 0.47±0.02, n= 216, K252a+GBZ 0.58±0.04, n=185; all significant differences <0.001, 2 Way ANOVA, no interaction, Tukey post test).

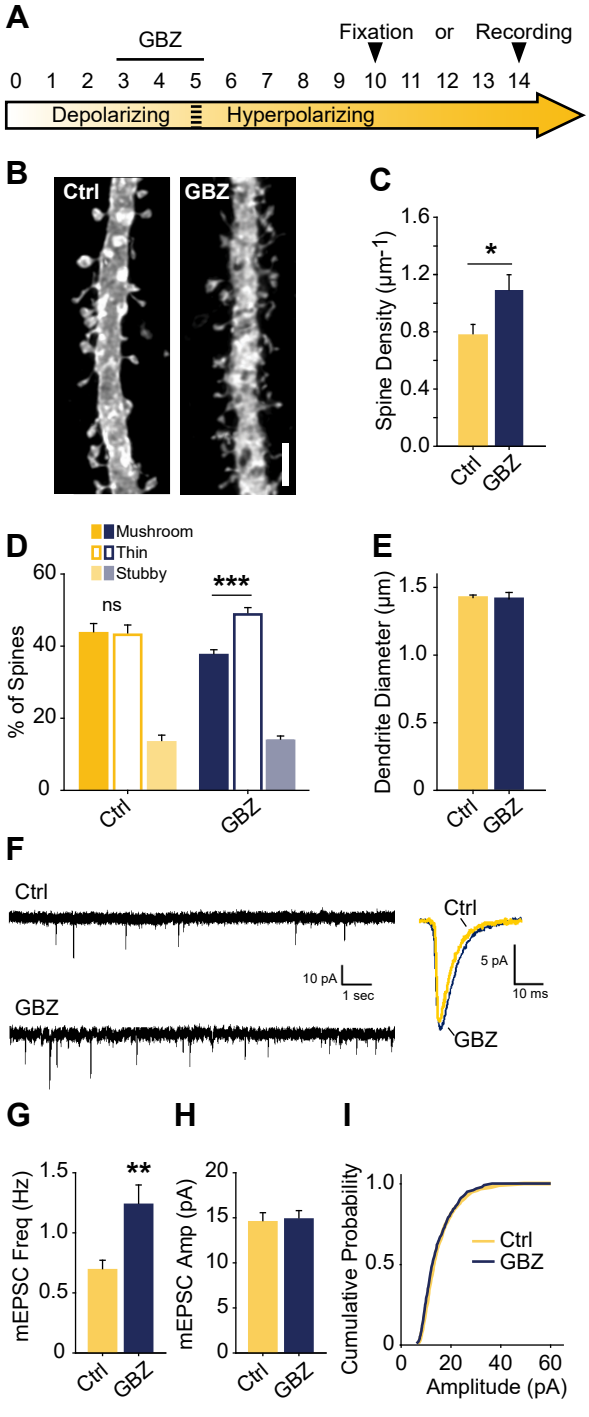
A
GBZ
Fixation or Recording
0 1 2 3 4 5 6 7 8 9 10 11 12 13 14
Depolarizing
Hyperpolarizing
B
Ctrl
GBZ
C
Spine Density (μm-1)
1.6
1.2
0.8
0.4
0.0
*
Ctrl
GBZ
D
Mushroom
Thin
Stubby
% of Spines
60
40
20
0
ns
***
Ctrl
GBZ
E
Dendrite Diameter (μm)
1.5
1.0
0.5
0
Ctrl
GBZ
F
Ctrl
10 pA
1 sec
GBZ
Ctrl
5 pA
10 ms
GBZ
G
mEPSC Freq (Hz)
1.5
1.0
0.5
0
**
Ctrl
GBZ
H
mEPSC Amp (pA)
20
15
10
5
0
Ctrl
GBZ
I
Cumulative Probability
1.0
0.5
0
Ctrl
GBZ
0 20 40 60
Amplitude (pA)

Figure 4

Figure 4. Transient blockade of depolarizing $GABA_A$ transmission causes a lasting increase in excitatory synapses and alters spine morphology. ***A,*** Schematic time course of GBZ treatment and experimental endpoints. ***B,C,*** Spine density after 3-5 DIV GBZ treatment and 5 days of recovery (Control 0.78±0.08 spines/µm, n=127; GBZ washout 1.07±0.07 spines/µm, n=112; N=6; p=0.024,). ***D,*** 3D spine morphology after 5 days of recovery (***p<0.001, critical level 0.05, Two Way ANOVA with Holm Sidak Post Test). ***E,*** Dendrite diameter after recovery (p=0.86). ***F,*** Representative mEPSC traces from slices after 8-9 days recovery. ***G,*** mEPSC frequency summary plot (Control: 0.70±0.08 Hz, n=10 GBZ: 1.23±0.17 Hz, n=10, p=0.009). ***H,*** mEPSC amplitude summary plot (Control: 14.50±1.07 pA, n=10, GBZ: 14.80±1.00 pA, n=10, p=0.84). ***I,*** Cumulative mEPSC distributions (p=0.58, Kolmogorov-Smirnov test). Scale bar 3µm.

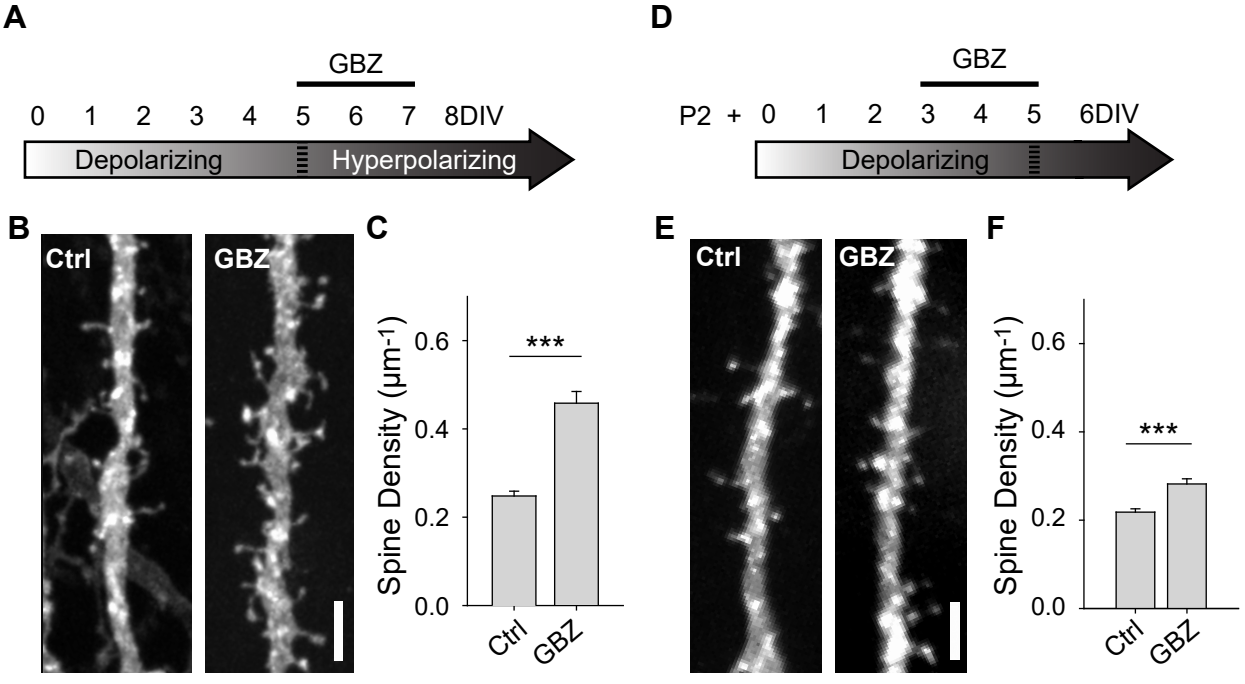

Supporting Figure 1

S1 Fig. GBZ-induced increase in spines is preserved in absence of antibiotics and in slices cultured from P2 mice. ***A,*** Time course of antibiotic-free GBZ treatment. ***B,C,*** Exemplary images and quantification of the spine enhancing effect of GBZ on slices cultures in antibiotic-free culture medium (Ctrl 0.248± 0.0109 μm^{-1}, n=198, GBZ 0.458±0.0264 μm^{-1}, n=70; N=4; p<0.001, Mann-Whitney). ***D,*** Time course of treatment of slices prepared from P2 pups. ***E,F,*** Exemplary images and quantification of spine enhancing effect of GBZ when applied to slices from P2 pups (Ctrl 0.22 ± 0.008 μm^{-1}, n=217, GBZ 0.28 ± 0.01 spines/μm^{-1}, n=156; N=3; p<0.001, Mann Whitney).

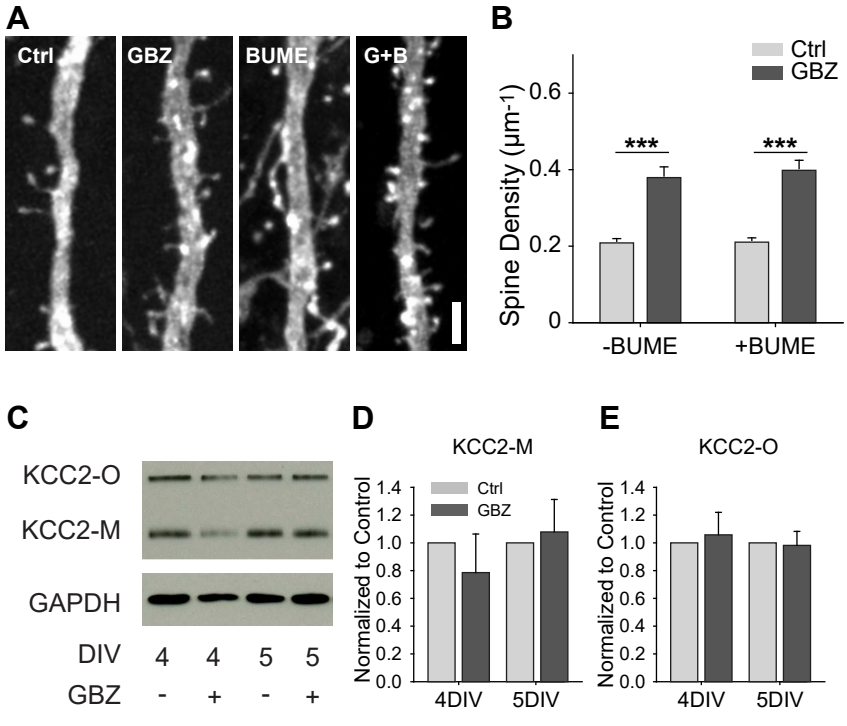

Supporting Figure 2

S2 Fig. GBZ-induced increase in spines is not reproduced by bumetanide and is not associated with changes in KCC2 expression. ***A***,***B***, Bumetanide does not increase spine density above control levels, (B, Control 0.21±0.01 um^{-1}, n=102; GBZ 0.38±0.02 um^{-1}, n=47; BUME 0.21±0.02 um^{-1}, n=88; BUME+GBZ 0.40±0.02 um^{-1}, n=53; N=3; Two-way ANOVA indicated no significant interaction between GBZ and BUME treatment (p=0.633). Tukey HSD post test indicates significant differences between Ctrl and GBZ in the absence of BUME (p<0.001) and in the presence of BUME (p<0.001)). ***C-E***, Western blot (C) showing no changes in monomeric (D) or oligomeric (E) KCC2 expression following GBZ from 3-4DIV (p=0.52 and 0.77, respectively, One Sample t-Test, n=3) and 3-5 DIV (p=0.76 and 0.87, respectively, One Sample t-Test, n=3). Scale bar 3µm.

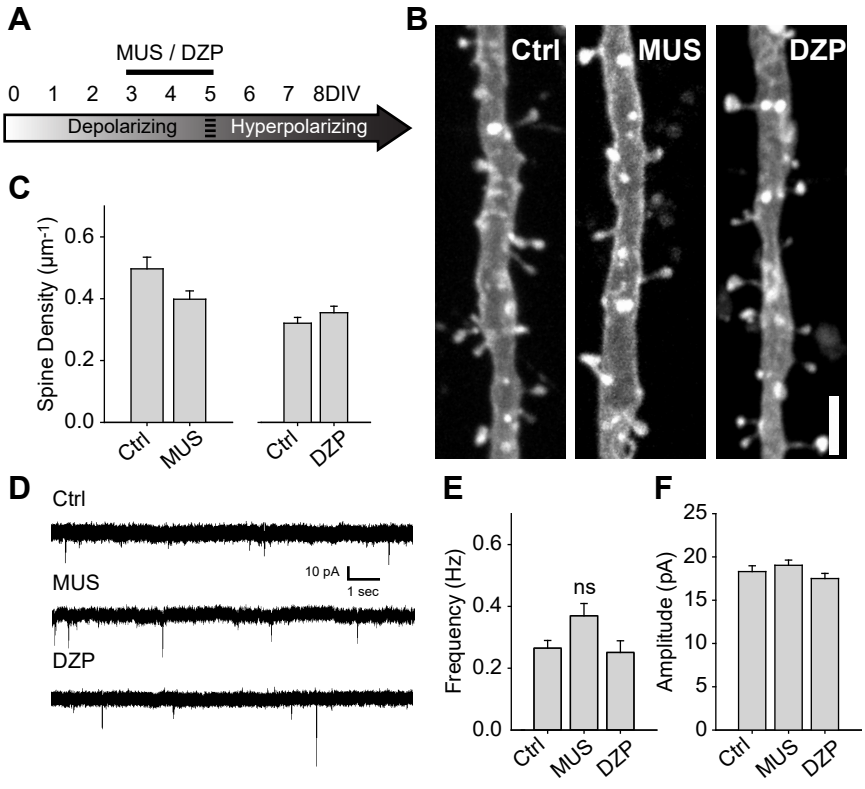

Supporting Figure 3

S3 Fig. Driving depolarizing $GABA_A$ transmission does not decrease glutamatergic synapse numbers. ***A,*** Time course of MUS and DZP treatment. ***B,C,*** Spine density after 3-5 DIV MUS treatment (Ctrl 0.50 ± 0.04, n=32; MUS 0.40 ± 0.03, n=39; N=7; p = 0.07) and DZP treatment (Ctrl 0.321 ± 0.02, n=116; DZP 0.36 ± 0.02, n=88; N=6; p = 0.11, Mann-Whitney). ***D,*** Representative traces of mEPSCs following 3-5DIV treatment with MUS or DZP. ***E,*** mEPSC frequency summary plot (Ctrl: 0.27 ± 0.02 Hz, n=9; MUS: 0.37 ± 0.04 Hz, n=8; DZP: 0.25 ± 0.04 Hz, n=8; One way ANOVA p=0.046; Ctrl vs MUS, p=0.09; Ctrl vs DZP, p=0.9). ***F,*** mEPSC amplitude summary plot (Ctrl: 18.3 ± 0.7 pA, n=9; MUS: 19.0 ± 0.6 pA, n=8; DZP: 17.5 ± 0.6 pA, n=8; One Way ANOVA, p=0.263)

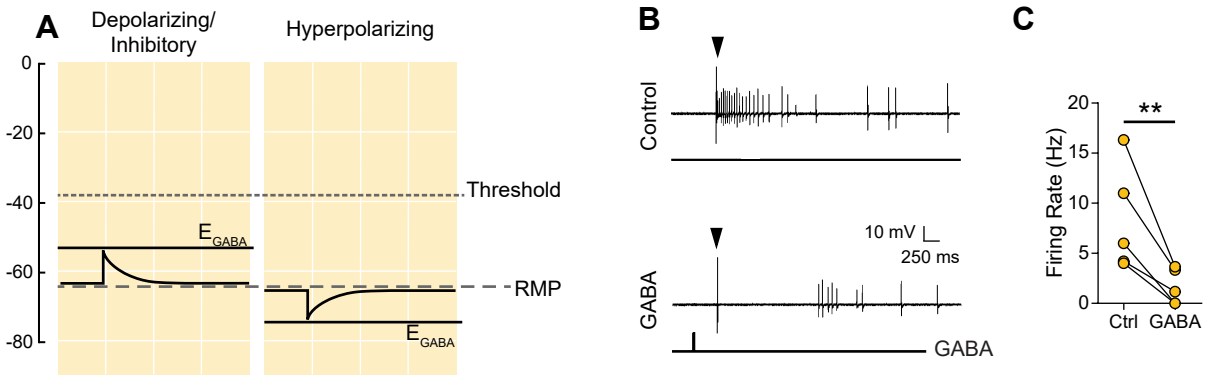

Supporting Figure 4

S4 Fig. Shunting GABA transmission inhibits electrically evoked firing in CA1 neurons at 3DIV. ***A,*** Schematic demonstrating the likely shunting and hence inhibitory nature of $GABA_A$ transmission due to the relative values of AP Threshold>E_{GABA}>RMP. The scale in A aligns with that of *Fig 1 E, F* and *G* such that the threshold, RMP and E_{GABA} values are represented accurately relative to each other. ***B,*** Sample traces from the same cell demonstrating that activity could be evoked electrically (Control) and that puffed GABA inhibited electrically evoked activity (GABA). The arrow above the traces denotes the timing of electrical stimulation. ***C,*** Summary plots of electrically evoked activity in the absence and presence of puffed GABA.

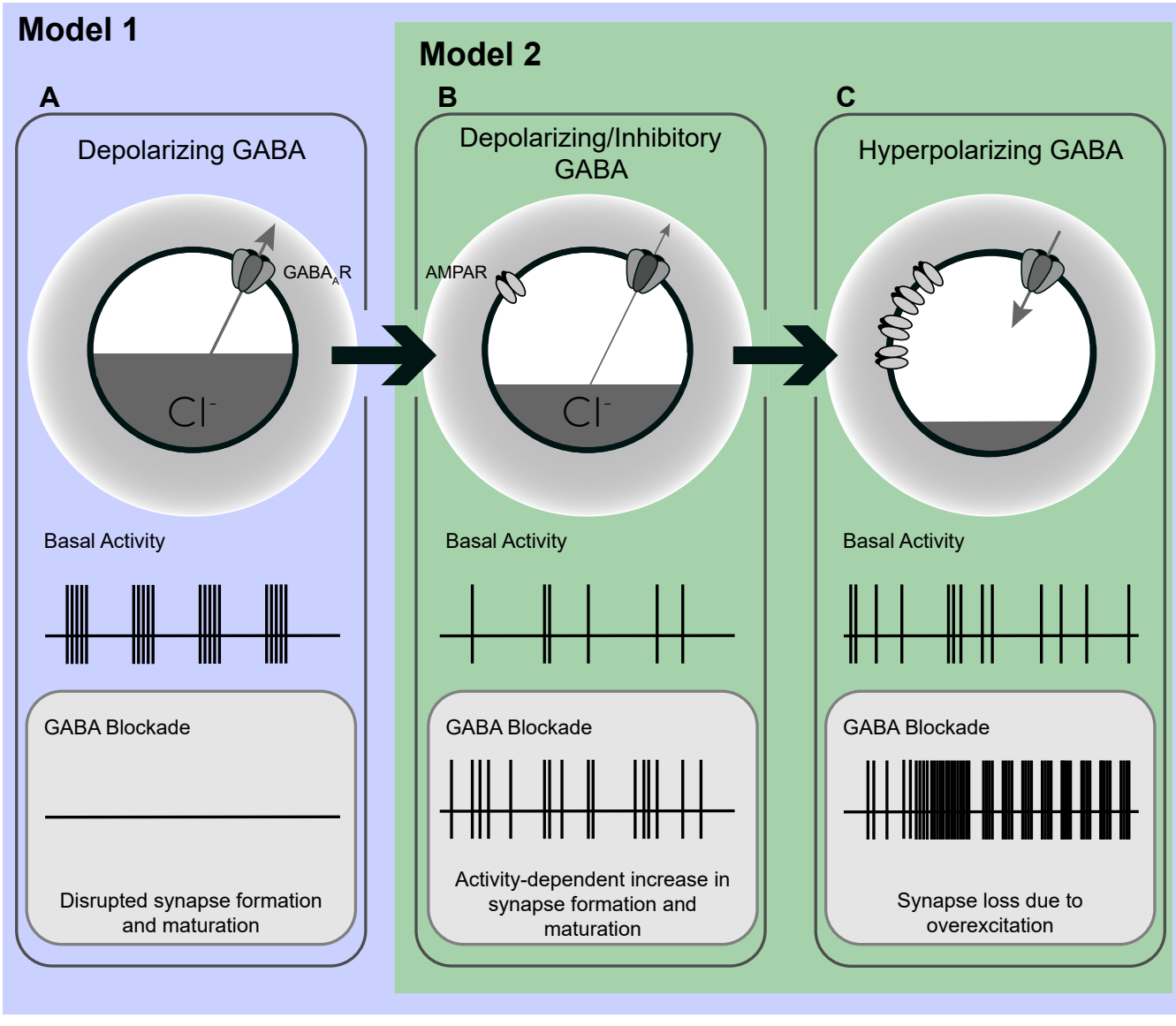

Supporting Figure 5

S5 Fig. A model of the possible roles of $GABA_A$ transmission in glutamatergic synapse formation as chloride homeostasis matures. ***A,*** Work performed in acute slices suggests that depolarizing $GABA_A$ transmission provides the initial excitatory drive required for activity- and calcium-dependent formation and maturation of glutamatergic synapses. Blocking $GABA_A$ transmission at this stage eliminated GDPs. For the sake of simplicity we have depicted that $GABA_A$ blockade would eliminate GDPs and silence network activity at this stage, however it should be noted that in acute slices, blocking $GABA_A$ transmission at this point has been shown to decrease circuit activity in immature acute hippocampal slices as depicted (Ben-Ari et al., 1989; Garaschuk et al., 1998; Mohajerani and Cherubini, 2005), but has also been shown to induce interictal discharges (Khazipov et al., 1997; Khalilov et al., 1999; Lamsa et al., 2000) or paroxysmal activity (Wells et al., 2000). These latter effects may be due to an overarching inhibitory role for GABA during development. ***B,*** Our work suggests a possible transition state wherein blocking $GABA_A$ transmission alleviates a depolarizing but inhibitory restraint on circuit activity, allowing for activity dependant formation of glutamatergic synapses. Such a transition state would likely rely on a still underdeveloped glutamatergic system that is not yet capable of pathological levels of overexcitation. Importantly, recent *in vivo* work suggests that GABA may be inhibit circuit activity throughout postnatal development, indicating that blocking $GABA_A$ transmission might enhance glutamatergic synapse formation from birth until GABA becomes fully hyperpolarizing. (Although the basal activity here is depicted as uncoordinated to clearly differentiate A from B, the activity pattern in this transition state, as well as in C, may very well be composed of ENOs.) ***C,*** When E_{Cl} and the glutamatergic system are mature, blocking hyperpolarizing $GABA_A$ transmission causes overexcitation and loss of glutamatergic synapses.